Kinetics of exciplex formation/dissipation in reaction following Weller Scheme II

ARTICLE *in* THE JOURNAL OF CHEMICAL PHYSICS · SEPTEMBER 2014

Impact Factor: 2.95 · DOI: 10.1063/1.4895625 · Source: PubMed

2 AUTHORS:

S. G. Fedorenko

Russian Academy of Sciences

26 PUBLICATIONS **204** CITATIONS

SEE PROFILE

Anatoly Israel Burshtein

Weizmann Institute of Science

216 PUBLICATIONS **3,131** CITATIONS

SEE PROFILE

THE JOURNAL OF PHYSICAL CHEMISTRY C

Article

pubs.acs.org/JPCC

Magnetic Field Effects in Fluorescence of Exciplex and Fluorophore for the Weller Schemes I and II: Similarities and Differences

Serguei V. Feskov

Volgograd State University, University Avenue, 100, Volgograd 400062, Russia

Anatoly I. Burshtein

Weizmann Institute of Science, Rehovot 76100, Israel

Anatoly I. Ivanov*

Volgograd State University, University Avenue, 100, Volgograd 400062, Russia

ABSTRACT: In exciplex-forming donor−acceptor systems the photoexcited acceptor state can be quenched either by exciplex formation at the contact of the acceptor and the donor, followed by reversible dissociation to the radical-ion pair (Scheme I), or by distant electron transfer yielding a radical-ion pair that can reversibly recombine to produce an exciplex (Scheme II). The fluorescence of the photoexcited electron acceptor (fluorophore) and the exciplex is known to be sensitive to the magnetic field, assisting spin conversion in the resulting geminate radical-ion pair (RIP). An increase of the fluorescence yield in high magnetic fields compared to low fields is known as the magnetic field effect (MFE). In this paper theories of the MFE on both the fluorophore and the exciplex within the Schemes I and II are developed. Kinetics of the reversible reactions are described in terms of the integral encounter theory that unlike the differential encounter theory is capable of dealing with such reactions. Regions of the parameters where MFE is observable are discussed. Comparison of functional dependencies of MFE on the model parameters for the Schemes I and II is carried out. Magnitudes and dependencies of MFE on the model parameters are found to be very similar for the Schemes I and II, except the dependencies of the fluorophore and exciplex MFEs on the rate constant of exciplex production from the radical-ion pair, which appear to be opposite for the Schemes I and II.

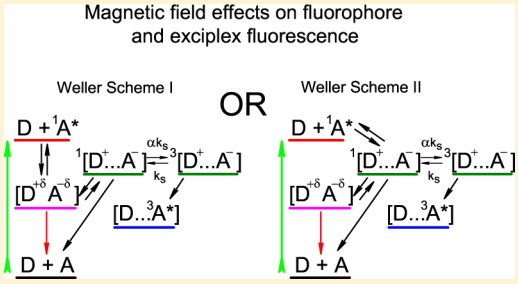

I. INTRODUCTION

Electron transfer (ET), being the simplest and a widespread reaction in artificial and biological systems, has been extensively investigated for several decades.[1−5] These investigations not only have provided an understanding of bimolecular photoinduced reactions but also have uncovered a series of promising applications, among them organic solid-state photovoltaic and other molecular optoelectronic devices.[6−10] Great efforts to study these processes have resulted in a deep understanding of the physical processes accompanying the charge transfer in solutions. Nevertheless, some important questions are still to be answered. Among them is the question in which sequence radical-ion pairs (RIPs) and exciplexes are formed in photoinduced electron transfer.[11−16] Exciplexes composed of a strongly coupled pair of the partially charged donor, $D^{+\delta}$, and the acceptor of the electron, $A^{-\delta}$, are produced in many photochemical reactions and manifest themselves through their specific fluorescence that allows monitoring their population kinetics. Besides, the exciplex fluorescence is sensitive to the external magnetic field, which is known as the magnetic field effect (MFE).

MFE in chemical reactions with radical-forming stages has received considerable attention in the last decades.[19−28] It is a common point of view now that the magnetic-sensitive stages of these reactions involve singlet−triplet transformations in RIPs. From the singlet precursor, the geminate RIP is initially produced in its singlet state due to conservation of the overall spin,[19] but when the distance between the RIP partners in solution becomes sufficiently large and their exchange coupling weakens, the hyperfine interaction can induce coherent singlet−triplet transitions in it. The external magnetic field, lifting the $S-T_{\pm}$ degeneracy to a sufficient extent, can significantly suppress singlet-to-triplet transformations in RIPs because only one $S-T_0$ conversion channel of three remains operative. This results in a slower rate of singlet−triplet conversion in strong magnetic fields (for organic systems, on the order of tens of millitesla). Because the part of the RIPs remaining in the singlet state in this case is larger, their

Received: July 15, 2014
Revised: August 21, 2014
Published: August 22, 2014

dx.doi.org/10.1021/jp5070648 | J. Phys. Chem. C 2014, 118, 21365−21376

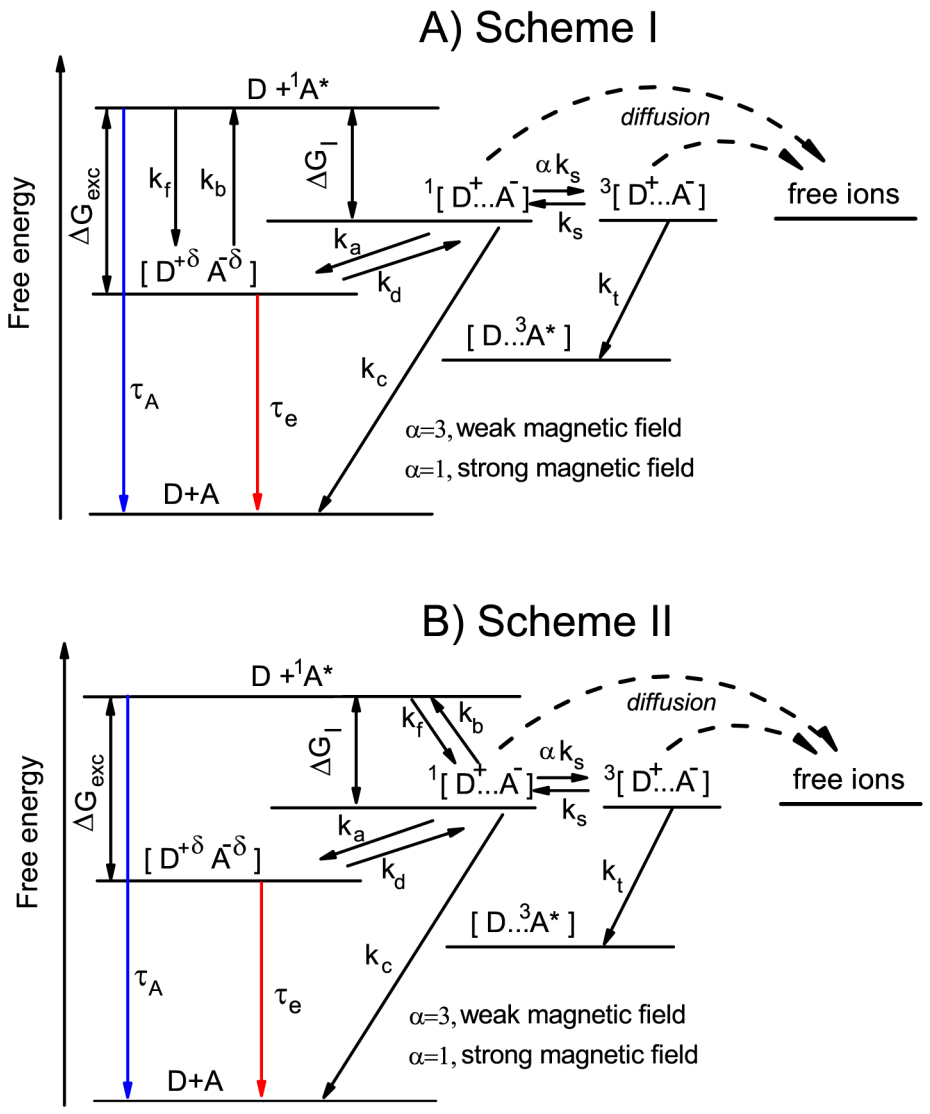

Figure 1. (A) Weller scheme I. Exciplexes are created directly from fluorophores and reversibly dissociate into radical-ion pairs (RIPs). (B) Weller scheme II. Exciplexes are created from RIPs, produced by reversible charge separation in the excited precursors A* + D. Designations of the rate constants are presented in both panels.

recombination reproducing exciplexes becomes more effective, and the quantum yield of the exciplex fluorescence increases. This is the so-called radical pair mechanism of the MFE.[29]

The MFE on the fluorophore fluorescence was detected rather recently,[18,28] while the MFE on the exciplex fluorescence has been known for a long time.[17] The magnitude of the effect on the fluorophore was found to be several times smaller than that on the exciplex. The MFE on the fluorophore as well as on the exciplex is transferred from the RIP due to the reversibility of mutual transformations of the fluorophore, exciplex, and RIP.[18] The magnitude of MFE strongly depends on dielectric permittivity of the solvent, ε, being small in both extremes of small and large values of ε and having a pronounced maximum in between.[18,25]

In quenching of photoexcitation by ET, an exciplex can be produced in two different ways known as the Weller Schemes I and II.[11,12,18,30−34] According to the Scheme I the exciplex formation occurs at the contact of the excited electron acceptor and the donor, followed by reversible dissociation to the radical-ion pair[30,31]

$$A + D \xrightarrow{h\nu} A^* + D \overset{\text{Diffusion}}{\longleftrightarrow} A^{-\delta}D^{+\delta} \leftrightarrow [A^- + D^+] \overset{\text{Diffusion}}{\longleftrightarrow} \text{free ions}$$

As indicated in the scheme, the geminate RIPs can separate into free ions due to mutual diffusion. On the other hand, Scheme II can be thought of as a distant electron transfer from the donor to the excited acceptor producing directly the ions, D^+ and A^-, which can reversibly form an exciplex during their encounters[32−34]

$$A + D \xrightarrow{h\nu} A^* + D \overset{\text{Diffusion}}{\longleftrightarrow} \underset{\downarrow\text{Diffusion}}{[A^- + D^+]} \overset{\text{Diffusion}}{\longleftrightarrow} A^{-\delta}D^{+\delta}$$
$$\text{free ions}$$

Generally, exciplexes and RIPs are generated in parallel,[33,35,36] and a reversible transition between them is possible.[37]

Recently the first investigations shedding light on the formation sequence of exciplexes and RIPs have appeared.[38,39] Making use of a combination of ultrafast spectroscopic techniques, including time-resolved infrared absorption, it was shown that in solvents of moderate polarity, like tetrahydrofuran, the ion pairs with low driving force are almost exclusively generated upon dissociation of the exciplex and that their

dx.doi.org/10.1021/jp5070648 | J. Phys. Chem. C 2014, 118, 21365−21376

recombination also occurs with the exciplex as an intermediate (Scheme I).[39] In addition, investigation of the time-resolved MFE in the exciplex-forming organic donor−acceptor systems evidenced that both the exciplex and the RIP are formed during the initial quenching stage (Schemes I and II are realized in parallel).[38] For the fluorophore/quencher pair 9,10-dimethylanthracene/*N*,*N*-dimethylaniline upon increasing the solvent polarity, the relative importance of the distant electron transfer quenching increases. However, even in comparably polar media, the exciplex pathway remains remarkably significant.[38]

Supposing the RIP and the exciplex formation proceed in accordance with the Scheme I, a theory of MFE on both the fluorophore and the exciplex is developed in refs 40−42 based on the models of incoherent and coherent spin evolution in RIPs. The reaction kinetics are described in terms of the integral encounter theory (IET) that unlike the differential encounter theory and its extension unified theory[43] is capable of dealing with the reversible reactions.[43−47] The theory[40−42] describes well the experimentally observed dependence of MFE magnitude on both the fluorophore and exciplex fluorescence on dielectric permittivity and viscosity of the solvent.[18,25,48]

The purposes of this paper are (i) to develop a theory of MFE on both the fluorophore and the exciplex fluorescence for the Schemes I and II in the framework of IET; (ii) to elicit the regions of the parameters where MFEs are observable; (iii) to compare functional dependencies of MFEs on model parameters for the Schemes I and II with the aim to distinguish which of them is realized in photochemical systems. The calculations are performed in the framework of the contact approximation for all reactions. For the Scheme I this approach seems to be undoubtedly proven, while the Scheme II explicitly supposes the fluorescence quenching by distant electron transfer.[32] To justify the contact approximation for such reactions it should be mentioned that in exciplex forming reactions the charge separation free energy gap does not exceed 0.5 eV. In this case the initial RIP distribution over the interion distances is adjacent to the contact and rather narrow,[49] so one can expect not too large a difference between predictions of the contact and noncontact models. To quantify this conclusion in Section VI we investigate the MFE dependence on width of the initial RIP distribution over the interion distances and clarify the area of the contact model applicability.

II. INTEGRAL ENCOUNTER THEORY FOR THE REVERSIBLE SEQUENTIAL REACTIONS OF EXCIPLEX AND RADICAL-ION PAIR FORMATION

We use a kinetic description for the reaction sequences presented in Figure 1 (the rate constants are indicated therein) and employ the conventional IET as a mathematical basis for our model.[43] According to the reaction schemes in panels A and B in Figure 1, we introduce the time-dependent populations of the fluorophore, $N^*(t)$, and the exciplex intermediate, $N_e(t)$.

In general the fluorescence in diluted solutions has well-separated short-lived and delayed components. The delayed fluorescence results from the ion encounters in the bulk and typically proceeds on the microsecond time scale. Here we restrict ourselves to the short-lived fluorescence, so we consider only the geminate processes. The full set of integral equations for the populations accounting for bulk recombination of ions is presented in refs 45 and 47. The reduced integral equations for the populations $N^*(t)$ and $N_e(t)$ accounting only for the geminate ion recombination we borrow from refs 40 and 47. They are

$$\frac{dN^*}{dt} = -c\int_0^t R_{11}(t-\tau)N^*(\tau)\mathrm{d}\tau + \int_0^t R_{12}(t-\tau)N_e(\tau)\mathrm{d}\tau - \frac{N^*}{\tau_A} \tag{1a}$$

$$\frac{dN_e}{dt} = c\int_0^t R_{21}(t-\tau)N^*(\tau)\mathrm{d}\tau - \int_0^t R_{22}(t-\tau)N_e(\tau)\mathrm{d}\tau - \frac{N_e}{\tau_e} \tag{1b}$$

where c is the concentration of the quencher ($c = [D] \gg [N^*]$), and τ_A and τ_e are the time constants of luminescence decay of the excited acceptor, A*, and of the exciplex in the absence of the reactions, correspondingly. These equations should be solved with the initial conditions

$$N^*(0) = N_0, \quad N_e(0) = 0 \tag{2}$$

that correspond to experiments with a short-pulse excitation of the fluorophore.

In the contact approximation the Laplace transform of the IET kernel (memory matrix) $\tilde{\hat{R}}(s)$ can be expressed through the matrix of the reaction rate constants, $\hat{K}$, and the reaction-free matrix Green function of the fluorophore quencher and radical-ion pairs $\hat{G}(\sigma|\sigma,t)$[45] at the contact distance σ

$$\tilde{\hat{R}}(s) = \hat{K}[\hat{E} - \hat{G}(\sigma|\sigma, s)\hat{K}]^{-1} \tag{3}$$

Here $\hat{E}$ is the identity matrix, and $\hat{G}(\sigma|\sigma, s)$ is the Laplace transform of $\hat{G}(\sigma|\sigma, t)$.[50]

To calculate the kernels the following collective basis has to be used[47]

$$\begin{pmatrix} {}^1\mathrm{A}^*\mathrm{D} \\ (A^{\delta-}\mathrm{D}^{\delta+}) \\ (\mathrm{A}^-\mathrm{D}^+)_S \\ (\mathrm{A}^-\mathrm{D}^+)_T \end{pmatrix} \tag{4}$$

The time-dependent Green function $G(r|r_0,t)$, accounting for the contact reactions, intraparticle relaxation, and spin transitions, obeys the following diffusional equation

$$\left(\frac{\partial}{\partial t} - \hat{L} - \hat{Q}\right)G(r|r_0, t) = \frac{\delta(r-r_0)}{4\pi r r_0}\delta(t)\hat{E} \tag{5}$$

where the diffusional operator

$$\hat{L} = \begin{pmatrix} L & 0 & 0 & 0 \\ 0 & 0 & 0 & 0 \\ 0 & 0 & L_c & 0 \\ 0 & 0 & 0 & L_c \end{pmatrix} \tag{6}$$

has two nonzero elements

$$L = \frac{D}{r^2}\frac{\partial}{\partial r}r^2\frac{\partial}{\partial r}, \quad L_c = \frac{D}{r^2}\frac{\partial}{\partial r}r^2 e^{r_c/r}\frac{\partial}{\partial r}e^{-r_c/r} \tag{7}$$

where L is the operator of free encounter diffusion for the neutral reactants ^{1}A* and ^{1}D, and L_c is the operator of encounter diffusion of RIPs subjected to Coulomb attraction. The diffusion coefficient D is considered to be the same for the

dx.doi.org/10.1021/jp5070648 | J. Phys. Chem. C 2014, 118, 21365−21376

neutral and the charged reactants; $r_c = e^2/(\varepsilon k_B T)$ is the Onsager radius; ε is the static dielectric permittivity of the solvent; k_B is the Boltzmann constant; and T is the bath temperature.

The relaxation matrix is composed of the rates of the excited acceptor and the exciplex fluorescence decay, $1/\tau_A$ and $1/\tau_e$, as well as of the rates of RIP spin transitions. Here the balance scheme of $S-T$ transitions is exploited to model dynamic $S-T$ transitions due to hyperfine couplings. Spin transitions in RIPs are described phenomenologically by the rate constant k_s and the coefficient α that discriminates between the low and high magnetic fields

$$\hat{Q} = \begin{pmatrix} -1/\tau_A & 0 & 0 & 0 \\ 0 & -1/\tau_e & & 0 \\ 0 & & -\alpha k_s & k_s \\ 0 & 0 & \alpha k_s & -k_s \end{pmatrix} \tag{8}$$

It is assumed that in the low-field limit all the spin states are degenerate, while in the high-field limit the three triplet components are split, so only two states (S and T_0) remain in resonance. Therefore, spin transitions, for example, from the singlet state ($\hat{Q}_{33} = -\alpha k_s$) proceed three times faster at $H \to 0$[49]

$$\alpha = \begin{cases} 3 & H \to 0 \\ 1 & H \to \infty \end{cases} \tag{9}$$

In low fields spin conversion equilibrates all 4 RIP substate populations leaving only 1/4 on the singlet one that exchanges with the exciplex. In the opposite limit the singlet population increases twice leaving the highly split triplet states $T_{\pm 1}$ almost empty. As a result, the back electron transfer from the RIP singlet state forms first the exciplex, and then the fluorophore is stronger in high magnetic fields.

Unlike $\hat{L}$ and $\hat{Q}$, the matrix of contact reactions $\hat{K}$ takes different forms within the Schemes I and II because the sequence of the exciplex/radical-ion pair reactions in these schemes differs. Here we focus on the Scheme II, taking into account that contact IET for the Scheme I was developed earlier in ref 40. Thus, the $\hat{K}$ matrix for the Scheme II has the following form in basis used

$$\hat{K} = \begin{pmatrix} -k_f & 0 & k_b & 0 \\ 0 & -k_d & k_a & 0 \\ k_f & k_d & -k_a - k_b - k_c & 0 \\ 0 & 0 & 0 & -k_t \end{pmatrix} \tag{10}$$

In what follows we will investigate the MFE phenomenon as a function of solvent permittivity ε, energetic parameters of the photochemical system (ΔG_{exc} and ΔG_I), the diffusion coefficient D, and other model parameters. We cannot however always assume these parameters to be free since they relate to each other according to some physical laws. For example, the rate constants k_f and k_b, as well as k_a and k_d, obey the detailed balance principle. In the Scheme II this principle gives the relations

$$k_f = k_b \exp[-\Delta G_I/k_B T] \tag{11}$$

$$k_d = k_a \exp[(\Delta G_{exc} - \Delta G_I)/k_B T]/v \tag{12}$$

where $v = 4\pi\sigma^2\Delta r$ is the volume of the reaction layer attached to the contact radius.[51,52]

The dependence of the rate constant k_f on the free energy gap ΔG_I can be approximated by the Marcus equation[1]

$$k_f = A \exp\left[-\frac{(\Delta G_I + E_{rm})^2}{4E_{rm}k_B T}\right] \tag{13}$$

Here E_{rm} is the energy of solvent reorganization caused by electron transfer. Since the exciplexes are observed only in low-exergonic electron transfer reactions, one could imply the inequality $|\Delta G_I| \ll E_{rm}$ to be fulfilled. In this case eq 13 can be rewritten in a simpler form

$$k_f = k_{f0} \exp\left[-\frac{\Delta G_I}{2k_B T}\right], \quad k_{f0} = A \exp\left[-\frac{E_{rm}}{4k_B T}\right] \tag{14}$$

which is used hereafter.

In Figure 1A the free energies of the exciplex formation from the neutral precursors ΔG_{exc} and of the RIP production ΔG_I are shown to be negative. These quantities can however essentially vary for different molecular systems and even change their sign. In what follows we study how MFE depends on the free energy levels of the exciplex and RIP. The rates of RIP recombination from the singlet state k_c and from the triplet states k_t are also added to the model to account for the recombination processes properly.

In many photochemical systems there is some correlation between the free energy changes ΔG_{exc} and ΔG_I. According to refs 53 and 54 the inequality $\Delta G_I - \Delta G_{exc} > 0$ is held. In particular, the enthalpy of formation of the exciplexes is substantially negative even at positive ΔG_I.[54] On the other hand, variation of the difference $\Delta G_I - \Delta G_{exc}$ from positive to negative values with increasing the solvent polarity ε was also reported.[55] This aspect is not considered in this paper, and the positive value of this difference is supposed. In such a case the exciplex formation rate k_a is expected to be a slowly varying function of $\Delta G_{exc} - \Delta G_I$. In calculations k_a is assumed to be independent of this parameter.

III. KERNELS OF INTEGRAL EQUATIONS IN CONTACT APPROXIMATION

A. Scheme II. Solution of eq 5 in the contact approximation has the following form (the Laplace transform)

$$\hat{G}(\sigma|\sigma, s) = \begin{pmatrix} g_f & 0 & 0 & 0 \\ 0 & 0 & 0 & 0 \\ 0 & 0 & (\alpha g_1 + g_0)/(\alpha+1) & (g_0 - g_1)/(\alpha+1) \\ 0 & 0 & \alpha(g_0 - g_1)/(\alpha+1) & \alpha(g_0 - g_1)/(\alpha+1) \end{pmatrix} \tag{15}$$

where $g_f = \tilde{G}_0(s + 1/\tau_A)$, $g_0 = \tilde{G}_c(s)$, and $g_1 = \tilde{G}_c(s + k_s(\alpha+1))$.

Here $\tilde{G}_0(s)$ is the Laplace transform of the reaction-free Green function for the diffusing neutral reactants

$$\tilde{G}_0(s) = \frac{1}{k_D}\frac{1}{1 + \sqrt{s\tau_d}} \tag{16}$$

where $k_D = 4\pi\sigma D$ is the diffusion rate constant of the contact reaction, while $\tau_d = (\sigma^2/D)$ is the effective encounter time for neutral partners.

On the other hand, $\tilde{G}_c(s)$ is the Laplace transform of the reaction-free Green function for the continuous diffusion in

dx.doi.org/10.1021/jp5070648 | J. Phys. Chem. C 2014, 118, 21365−21376

Coulomb potential. A close analytical approximation for this Green function was obtained in ref 56. It has the form

$$\tilde{G}_c(\sigma, \sigma, s) = \frac{1}{k_D} \cdot \frac{1}{\mu_0(x) + \kappa(x, s)} \tag{17}$$

where

$$\mu_0(x) = \frac{1/x}{\exp(1/x) - 1},$$
$$\kappa(x, s) = \frac{s\tau_d + [\nu(x)/\rho(x)]\sqrt{s\tau_d}}{\sqrt{s\tau_d} + \nu(x)},$$
$$\varrho(x) = x^2 \exp(1/x)[1 - \exp(-1/x)]^2$$

Here

$$\nu(x) = \left\{x^3[\exp(1/x) + \exp(-1/x) - 2] - x\right\} / \left\{\frac{1}{6}[Ei(1/x) - \exp(1/x)(x + x^2 + 2x^3)] + \frac{1}{6}[E_1(1/x) - \exp(-1/x)(x - x^2 + 2x^3)] + \frac{2}{3}x^3 + x\right\}$$

$x = \sigma/r_\sigma$, while Ei and E_1 are the integral exponential functions.

From eq 3 one gets the integral kernels $\tilde{R}_{ij}$ for the Weller Scheme II

$$\tilde{R}_{11} = k_f[\alpha + 1 + (\alpha g_1 + g_0)(k_a + k_c) + [\alpha g_0 + g_1 + (\alpha + 1)g_0 g_1(k_a + k_c)]k_t]/Y \tag{18}$$

$$\tilde{R}_{12} = k_b k_d[\alpha g_1 + g_0 + (\alpha + 1)g_0 g_1 k_t]/Y \tag{19}$$

$$\tilde{R}_{21} = \frac{k_f k_a}{k_b k_d}\tilde{R}_{12} \tag{20}$$

$$\tilde{R}_{22} = k_d\{(1 + g_f k_f)[1 + \alpha + (\alpha g_1 + g_0)k_c] + (\alpha g_1 + g_0)k_b + [(1 + g_f k_f)(a g_0 + g_1) + (1 + a)g_0 g_1(k_b + k_c(1 + g_f k_f))]k_t\}/Y$$

$$Y = (1 + g_f k_f)[1 + a + (a g_1 + g_0)(k_a + k_c)] + (a g_1 + g_0)k_b + [(1 + g_f k_f)(a g_0 + g_1 + (1 + a)g_0 g_1 (k_a + k_c)) + (1 + a)g_0 g_1 k_b]k_t \tag{21}$$

B. Scheme I. The same kernels can be calculated for the Scheme I. This was done earlier in ref 40, so we will borrow $\tilde{R}_{ij}$ expressions from there

$$\tilde{R}_{11} = \tilde{R}_{21} = \frac{k_f}{1 + g_f k_f} \tag{22}$$

$$\tilde{R}_{12} = \frac{k_b}{1 + g_f k_f} \tag{23}$$

$$\tilde{R}_{22} = \tilde{R}_{12} + k_d \left[1 - \frac{k_a[\alpha g_1 + g_0 + (\alpha + 1)g_0 g_1 k_t]}{\alpha + 1 + [\alpha g_1 + g_0 + (\alpha + 1)g_0 g_1 k_t](k_a + k_c) + (\alpha g_0 + g_1)k_t}\right] \tag{24}$$

It should be pointed out that k_b (as well as k_f) relates to different types of reactions within the Schemes I and II (compare Figures 1A and 1B). The quantity k_b describes the first-order (monomolecular) reaction in the Scheme I and the second order (bimolecular) reaction in the Scheme II. That is why the relation between k_b and k_f for the Scheme I takes the form

$$k_b = k_f \exp(-\Delta G_{exc}/k_B T)/\nu \tag{25}$$

On the other hand, the rate constants k_a and k_d describe the same type of reactions in both schemes, so that eq 12 holds for the Scheme I as well.

IV. FLUORESCENCE QUANTUM YIELDS AND MAGNETIC FIELD EFFECTS

Laplace transformations of eqs 1a and 1b allow us to find the quantum yield of the A* fluorescence

$$\eta_f = \frac{\tilde{N}^*(0)}{N_0\tau_A} = \frac{1}{1 + c\tau_A k_g} \tag{26}$$

where $\tilde{N}^*(s)$ is the Laplace transform of the fluorophore population kinetics $N^*(t)$ and k_g is easily expressed via the memory kernels $\tilde{R}_{ij}(s)$[47]

$$k_g = \tilde{R}_{11}(0) - \frac{\tilde{R}_{12}(0)\tilde{R}_{21}(0)}{\tilde{R}_{22}(0) + 1/\tau_e} \tag{27}$$

In a similar way one obtains the following expression for the quantum yield of the exciplex fluorescence[40,47]

$$\eta_e = \frac{\tilde{N}_e(0)}{N_0\tau_e} = \frac{c\tau_A\tilde{R}_{21}(0)\eta_f}{1 + \tilde{R}_{22}(0)\tau_e} = \frac{\tilde{R}_{21}(0)(1 - \eta_f)}{\tilde{R}_{11}(0) + \tau_e(\tilde{R}_{11}(0)\tilde{R}_{22}(0) - \tilde{R}_{12}(0)\tilde{R}_{21}(0))} \tag{28}$$

In weak external magnetic fields we will use the value $\alpha = 3$ and designate these quantities as η_f^w and η_e^w, correspondingly. In strong magnetic fields we will set $\alpha = 1$, designating the corresponding values as η_f^s and η_e^s. Then we define the MFE on the fluorophore as

$$\chi_f = \frac{\eta_f^s - \eta_f^w}{\eta_f^w} \tag{29}$$

while the MFE on the exciplex, accordingly

$$\chi_e = \frac{\eta_e^s - \eta_e^w}{\eta_e^w} \tag{30}$$

The last two equations yield rather simple analytical solution of the problem in the contact approximation.

V. SIMULATIONS OF THE MAGNETIC FIELD EFFECT

The model used incorporates a lot of parameters, so we reduce their number by fixing a part of them accepting some typical values. We set concentration of quencher molecules to c = 0.00003 Å^{-3} = 0.05 M, the diffusion coefficient D = 250 Å^2/ns, and the encounter radius (sum of the donor and acceptor radii)

dx.doi.org/10.1021/jp5070648 | J. Phys. Chem. C 2014, 118, 21365−21376

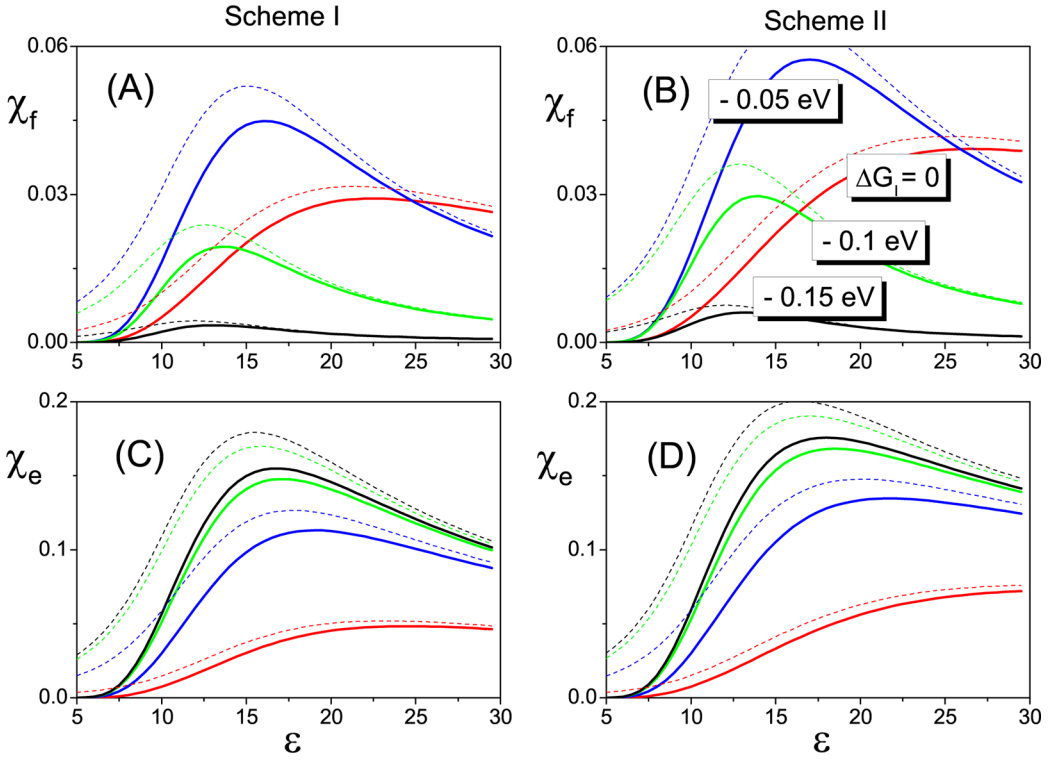

Figure 2. Magnetic-field effect on fluorophore χ_f and exciplex χ_e as a function of solvent permittivity ε. For the Scheme I the results are indicated on panels (A) and (C) and for the Scheme II on panels (B) and (D). Red, blue, green, and black curves correspond to $\Delta G_I = 0$, −0.05, −0.1, and −0.15 eV. Other parameters are $\tau_A = 5$ ns, $\tau_e = 50$ ns, $k_s = 0.03$ ns^{-1}, $k_a = 15\,000$ Å^3/ns, $D = 250$ Å^2/ns, $\Delta G_{exc} = \Delta G_I - 0.1$ eV, $k_f = 50\,000$ Å^3/ns (Scheme I), and $k_{f0} = 50\,000$ Å^3/ns (Scheme II).

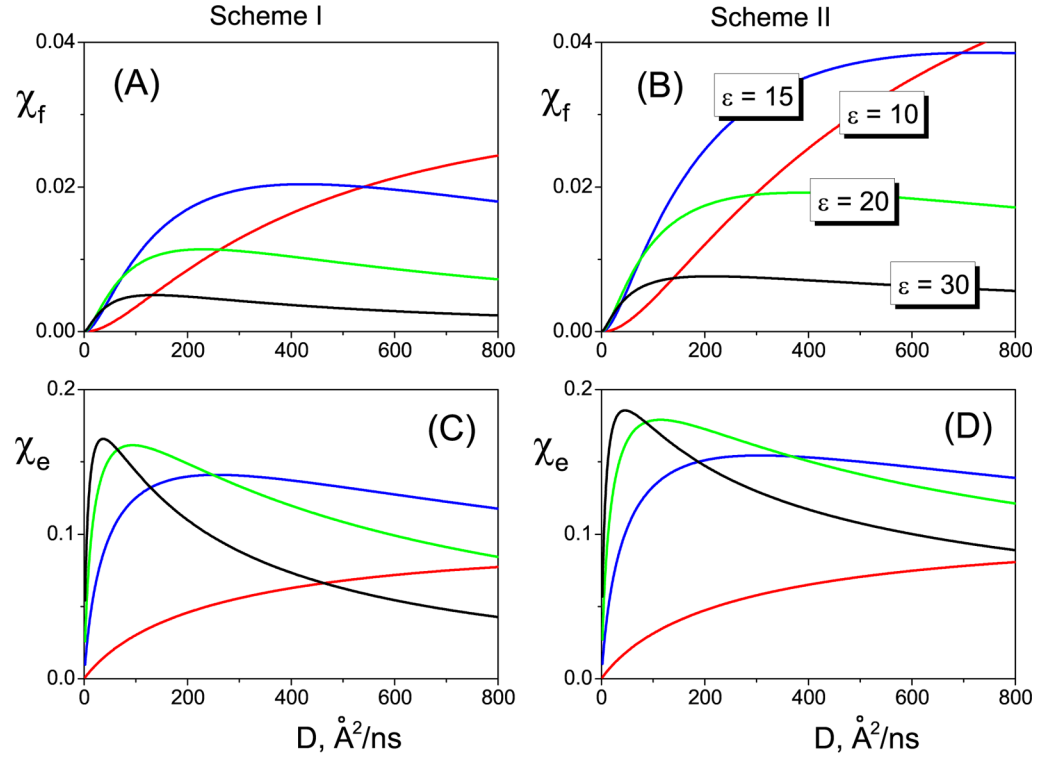

Figure 3. Magnetic-field effect on fluorophore χ_f and exciplex χ_e as a function of the RIP diffusion coefficient D for a few values of ε. Red, blue, green, and black curves correspond to $\varepsilon = 10$, 15, 20, and 30. Arrangement of the panels is the same as in Figure 2. Other parameters are $\tau_A = 5$ ns, $\tau_e = 50$ ns, $k_s = 0.03$ ns^{-1}, $k_a = 15\,000$ Å^3/ns, $\Delta G_{exc} = -0.2$ eV, $\Delta G_I = -0.1$ eV, $k_f = 50\,000$ Å^3/ns (Scheme I), and $k_{f0} = 50\,000$ Å^3/ns (Scheme II).

$\sigma = 6.85$ Å. The exciplex and the fluorophore lifetimes are $\tau_e = 50$ ns and $\tau_A = 5$ ns so that a typical value of the ratio $\tau_e/\tau_A = 10$ is kept.[36] The singlet−triplet transition rate in RIP is $k_s = 0.03$ ns^{-1}.[28] The rate constant of exciplex formation k_f is known to

dx.doi.org/10.1021/jp5070648 | J. Phys. Chem. C 2014, 118, 21365−21376

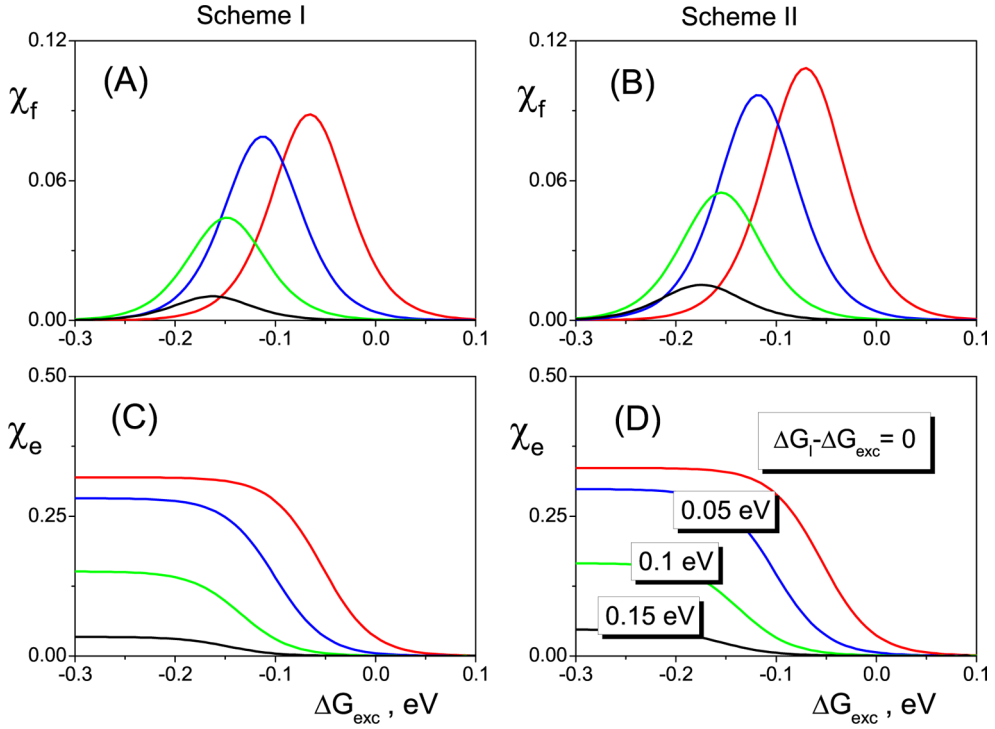

Figure 4. Magnetic-field effect on fluorophore χ_f and exciplex χ_e as a function of the free energy gap ΔG_{exc}. Arrangement of panels is the same as in Figure 2. Red, blue, green, and black curves correspond to $\Delta G_I - \Delta G_{exc}$ = 0, 0.05, 0.1, and 0.15 eV. Parameters used: ε = 15; others are the same as in the Figure 2 caption.

be close to the diffusion rate constant.[57] Since $k_D = 4\pi\sigma D$ = 21500 Å^3/ns for the accepted parameters, the value k_f = 50 000 Å^3/ns is used. It should be pointed out that MFE magnitudes depend weakly on this quantity.

The calculated ε-dependencies of MFE on the fluorophore and exciplex for both schemes are shown in Figure 2 for a few energy configurations. First we consider MFE in the absence of RIP recombination, $k_t = k_c = 0$ (solid lines). The distinguished feature of this dependence is the well-observed left boundary of the effect. In the low-polar solvent, $\varepsilon < 6$, the Coulomb well is so deep that RIPs are not able to separate at all and are predestined to transform back to either the exciplex or the fluorophore. This happens earlier or later at any spin-conversion rate, and therefore the fluorescence quantum yields are independent of αk_s which results in negligible MFEs. This conclusion is supported by the fact that at $\varepsilon < 6$ and $k_c = k_t = 0$ the total fluorescence yield $\eta_f + \eta_e \to 1$. The position of the left boundary for χ_f and χ_e is most sensitive to the value of the encounter radius σ. At σ = 3 Å, for example, it shifts to ε = 15.

The second feature is a pronounced similarity of the ε-dependencies of MFE for the first and second schemes. This is a direct consequence of three facts: (i) the MFE is formed at the RIP stage, (ii) only mutual motion of the radical ions is influenced by the solvent polarity, and (iii) the RIP evolution is the same for two schemes.

To demonstrate the influence of triplet state recombination on quantum yields of fluorescence, the $\chi_f(\varepsilon)$ and $\chi_e(\varepsilon)$ dependencies are presented in Figure 2 by dashed lines, calculated with the same parameters except for k_t that is set to 10^4 Å^3/ns. The triplet recombination rate constant, k_t, is known to be much larger than that of the singlet recombination[58] so we set $k_c = 0$. Variation of k_t from zero to 10^4 Å^3/ns leads to considerable increase of MFEs, χ_f and χ_e. To clarify the mechanism of this effect we note that RIP recombination to the ground or the triplet excited state of the fluorophore decreases the probability of exciplex and excited fluorophore production and, hence, decreases their fluorescence quantum yields in both strong and weak magnetic fields. The calculations show that the differences $\eta_f^s - \eta_f^w$ and $\eta_e^s - \eta_e^w$ (the nominators in eqs 29 and 30) are almost independent of k_t, while η_f^w and η_e^w (the denominator in eqs 29 and 30) considerably decrease with the rise of k_t. This is the reason why the magnitude of the MFEs increases with k_t. Therefore, all the dashed lines in Figure 2 representing MFEs at large k_t appear above the MFE curves at zero recombination rates (solid lines). Another manifestation of the strong triplet recombination is disappearance of the left boundary for MFEs (see dashed lines in Figure 2).

In many photochemical systems, the energetic and kinetic parameters, ΔG_{exc}, ΔG_I, τ_e, k_b, k_d, and k_a, depend on solvent polarity. Despite that the results presented in Figure 2 neglect these dependencies, the calculated $\chi_f(\varepsilon)$ and $\chi_e(\varepsilon)$ functions are very similar to those obtained in experiments.[18,37] This means that the ε-dependencies observed in experiments are mainly due to variation of the Coulomb attraction between the ions with ε influencing their mutual diffusion.

The diffusional dependencies of MFEs for the both schemes are shown in Figure 3 for a few values of ε. All curves have typical bell-shaped form, but not all of them achieve their maximum in the interval pictured in Figure 3. This can be easily understood, for example, for the Scheme I. For small D the probability of RIP association into exciplex is much larger than the probability of free ion formation; therefore, the RIP cannot avoid the association into the exciplex. In this case conversion of the exciplex into the RIP only terminates its fluorescence and transformation into a fluorophore. Some delay in the exciplex evolution caused by its temporary sojourn in the RIP state cannot change the exciplex fluorescence quantum yields. This means that the MFE should vanish in the limit $D \to 0$.

dx.doi.org/10.1021/jp5070648 | J. Phys. Chem. C 2014, 118, 21365−21376

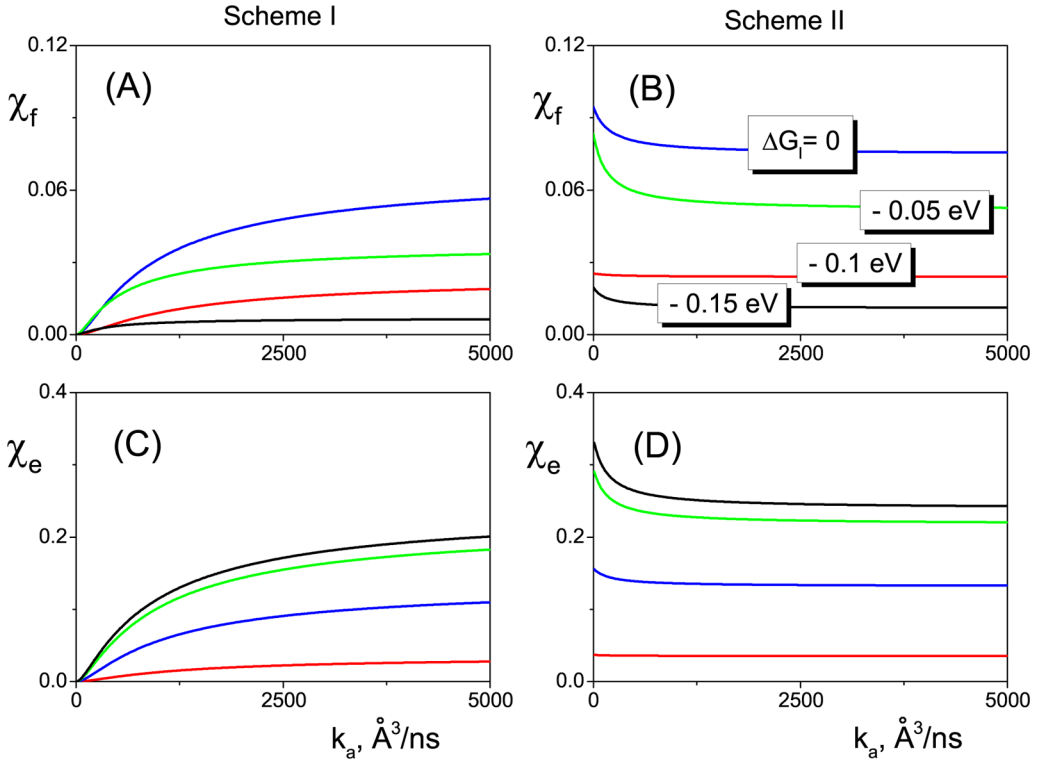

Figure 5. Magnetic-field effect on fluorophore χ_f and exciplex χ_e as a function of the RIP-to-exciplex association rate k_a. Arrangement of panels is the same as in Figures 2−4. Red, blue, green, and black curves correspond to ΔG_I = 0, −0.05, −0.1, and −0.15 eV. Parameters used: $\Delta G_I - \Delta G_{exc}$ = 0.075 eV, ε = 15; others are the same as in the Figure 2 caption.

In the opposite limit of large D the MFE is also negligible since the reaction $^1[D^{+\delta}A^{-\delta}] \rightarrow {}^1[D^+ + A^-]$ becomes irreversible and, hence, the singlet−triplet evolution of RIP cannot affect the fluorescence quantum yields of the exciplex. In this limit the probability of the free ion formation is much larger than the probability of RIP association into exciplex. So, the maximum of the MFE should be expected when the probabilities of free ion formation and RIP association into the exciplex are close to each other. This condition is fulfilled when the equation $\eta_e = (1 - \eta_f)/2$ is met. From this equation and eq 28 for $k_t = k_c = 0$ and $k_s = 0$ we obtain[42]

$$k_D = \frac{k_a}{\mu_0(\tau_e k_d - 1)} \tag{31}$$

This equation provides a rough estimation for the position of the MFE maximum. It should be noted that the bell-shaped curves are qualitatively similar to those obtained experimentally (see Figure 5 in ref 48). All curves demonstrate the maximum that shifts to smaller values of D with increasing ε (similarly in both schemes).

The dependence of the MFE on the free energy of exciplex formation, ΔG_{exc}, for a few values of the difference $\Delta G_I - \Delta G_{exc}$ is shown in Figure 4. One can see again a close similarity of the MFE behavior for two schemes. The $\chi_f(\Delta G_{exc})$ dependence has a rather narrow maximum and quickly vanishes for both large and small $-\Delta G_{exc}$, while the $\chi_e(\Delta G_{exc})$ monotonously rises with increasing $-\Delta G_{exc}$ reaching a plateau.

The behavior of both χ_f and χ_e is in qualitative accordance with the experimental results (see Figure 6 in ref 28). At the same time there are some quantitative differences: (i) the calculated maximum of χ_f lies in the interval 0.1−0.2 eV, while the experimental data show the maximum at $-\Delta G_{exc} \approx 0.4$ eV; (ii) the theory predicts the position of the right edge of the χ_e-plateau at $-\Delta G_{exc} \approx 0.1$−0.2 eV, while in experimental data χ_e rises up at $-\Delta G_{exc} \approx 0.5$ eV and does not achieve plateau in the experimental window. There are several reasons for these inconsistencies. First, the exciplex-to-RIP transformation is supposed to occur at the encounter radius σ = 6.85 Å, while the interplanar separation in exciplexes is estimated to be 3 Å.[11] Calculations show that a decrease of σ shifts the χ_f maximum and the right edge of the χ_e plateau to larger $-\Delta G_{exc}$. Second, except for ΔG_{exc}, all parameters are kept constant in calculations, but in real systems they can vary. At last, experimental values of ΔG_{exc} and ΔG_I are indirectly determined and can have some systematic errors.

Simulations have shown that the only parameter which influences the magnitude of MFE oppositely in the first and the second schemes is the exciplex association rate constant k_a. The $\chi_f(k_a)$ and $\chi_e(k_a)$ dependencies are pictured in Figure 5 for a few values of the ΔG_I parameter. The theory predicts a monotonous increase of both χ_f and χ_e with k_a for the Scheme I and a monotonous decrease for the Scheme II. For the vanishing k_a and k_d the RIPs in Scheme I are not produced at all (see eq 12) so the magnetic-sensitive stage of the reaction is absent. This is the reason for vanishing χ_f and χ_e in the limit $k_a \rightarrow 0$. As for the Scheme II, it has the magnetic field sensitive stage in this limit, but the exciplexes are not produced and $\eta_e \rightarrow 0$. As a result, at any nonzero k_a the exciplex production is magnetic sensitive, and MFEs, χ_f and χ_e, are not zero.

VI. THE EXCIPLEX MFE IN THE SCHEME II BEYOND THE CONTACT APPROXIMATION

Analytical expressions for the IET rate kernels eqs 18−24, used so far for the MFE analysis in both the quenching schemes (I

dx.doi.org/10.1021/jp5070648 | J. Phys. Chem. C 2014, 118, 21365−21376

and II), were derived within the contact approximation assuming all the ET processes in chemical system to proceed at collisions of the reacting particles in solution. Sometimes this contact approximation is not however valid, for example, in highly exergonic electron transfer processes in the Marcus inverted region, $-\Delta G_I > E_{rm}$ (with E_{rm} being the reorganization energy of the solvent). In this case the ET can be shifted out of the contact distance, so that the primary products of the reaction are the "loose" ion pairs with the mean interparticle distance considerably larger than the contact radius σ.[49]

Our treatment of the A* fluorescence quenching as a sequence of contact reactions can be questioned from this point of view. The most doubt here seems the first stage in the Scheme II, photoinduced initial separation of charges $A^* + D \rightarrow A^- + D^+$. In what follows we examine the applicability of the contact approximation here comparing the results of the present theory with numerical data obtained within the model accounting for electronic transitions between the remote partners. To simplify analysis we suppose here that initial charge separation proceeds irreversibly, so that the differential encounter theory (unified theory[49]) can be used to describe this process. In this limit the MFE on fluorophore vanishes, so in this section we will analyze only the exciplex MFE.

To estimate the effect of "distant" ET on the χ_e quantity within the Scheme II, we calculate the quantum yield of exciplexes $\overline{\eta}_e$ as a function of the electron tunnelling length L. This parameter determines the decay of electronic coupling $V_I(r)$ with increase of the A*−D distance r

$$V_I(r) = V_0 \exp\left[-\frac{r-\sigma}{L}\right] \tag{32}$$

where V_0 is the contact value of the coupling parameter. The rate of the photoinduced charge separation $A^* + D \rightarrow A^- + D^+$ then can be calculated as[4]

$$W_I(r) = V_I^2(r)\sqrt{\frac{\pi}{E_{rm}(r)k_BT}}\exp\left[-\frac{(\Delta G_I + E_{rm})^2}{4E_{rm}k_BT}\right] \tag{33}$$

Solvent reorganization energy E_{rm} changes with r according to the Marcus formula[1] $E_{rm}(r) = E_{rm}(\sigma)(2 - \sigma/r)$, while the free energy gap between A* + D and $A^- + D^+$ electronic levels is assumed to be constant, $\Delta G_I(r) = \Delta G_I(\sigma)$.

Using the unified theory of photochemical processes within the donor−acceptor molecular systems[49] one can calculate the initial distribution of RIPs over the interparticle distances as

$$m_0(r) = W_I(r)\int_0^\infty n(r, t)N^*(t)\mathrm{d}t \tag{34}$$

where $n(r,t)$ is the auxiliary function describing the distribution of reactants in solvent. This function obeys the equation

$$\frac{\partial n}{\partial t} = -W_I(r)n + Ln \tag{35}$$

with the initial and boundary conditions

$$n(r, t = 0) = 1, \quad \frac{\partial n}{\partial r}(r = \sigma, t) = 0 \tag{36}$$

On the other hand, the kinetics of the excited state population $N^*(t)$ is described by the equation

$$\dot{N}^* = -ck_I(t)N^* - N^*/\tau_A, \quad k_I(t) = \int_\sigma^\infty W_I(r)n(r, t)\mathrm{d}^3r \tag{37}$$

with the initial condition $N^*(0) = 1$.

The quantum yield of the exciplexes $\overline{\varphi}_e$ within the Weller Scheme II can be found by averaging the partial yields $\varphi_e(r)$ over the distances between the RIP partners

$$\overline{\varphi}_e = c\int \varphi_e(r)m_0(r)\mathrm{d}^3r \tag{38}$$

By definition, $\varphi_e(r)$ is the probability to form an exciplex from the ion pair initially separated by distance r. This quantity was derived earlier in ref 49 (see P. 572). We borrow the corresponding expression from this paper

$$\varphi_e(r) = K\left\{\frac{\tilde{G}_c(\sigma, r, 0)}{1 + K^\#\tilde{G}_c(\sigma, \sigma, 0)} - \tilde{\rho}_{ST}(\sigma, r, 0)\left[1 + \frac{(k_t - K^\#)\tilde{G}_c(\sigma, \sigma, 0)}{1 + K^\#\tilde{G}_c(\sigma, \sigma, 0)}\right]\right\} \tag{39}$$

where $K = k_a/(1 + k_d\tau_e)$ is the rate of exciplex formation from RIP, $K^\# = K + k_c$, and $G_c(\sigma,r,t)$ is the Green function for spatial diffusion in the Coulomb potential.

Instead of the contact Green function $\tilde{G}_c(\sigma,\sigma,s)$ used in Section III, here we need a more general expression for $\tilde{G}_c(\sigma,r,s)$ which would be accurate for $r > \sigma$. Several approximations for the noncontact Green function in Coulomb potential are well-known from the literature, and the areas of their applicability are discussed in refs 59−61. In this study we use a rather simple expression for $\tilde{G}_c(\sigma,r,s)$ which is accurate for high-permittivity solvents ($r_c \leq 10$ Å). Using the designation $r_e = r_c/(1 - e^{-r_c/r})$ for the effective radius, this expression can be written as[61]

$$\tilde{G}_c(\sigma, r, s) = \exp\left(\frac{r_c}{\sigma}\right)\frac{\exp(-r_c/2\sqrt{s/D}\,[\coth(r_c/2r) - \coth(r_c/2\sigma)])}{4\pi D r_e(r)[1 + r_e(\sigma)\sqrt{s/D}\,]} \tag{40}$$

The analytic expression for the $\tilde{\rho}_{ST}(\sigma,r,s)$ in eq 39 varies depending on the model of the singlet−triplet transitions in RIPs. In the case of low magnetic fields it has the form

$$\tilde{\rho}_{ST}(\sigma, r, s) = 3k_s\frac{\tilde{J}_c(r, s)[1 + K^\#\tilde{G}_c(\sigma, \sigma, s)] - \tilde{J}_c(\sigma, s)K^\#\tilde{G}_c(\sigma, r, s)}{1 + 3k_sk_t\tilde{J}_c(\sigma, s) + K^\#[\tilde{G}_c(\sigma, \sigma, s) - 3k_s\tilde{J}_c(\sigma, s)]} \tag{41}$$

where the auxiliary function

$$\tilde{J}_c(r, s) = \frac{\tilde{G}_c(\sigma, r, s) - \tilde{G}_c(\sigma, r, s + 4k_s)}{4k_s[1 + k_t\tilde{G}_c(\sigma, \sigma, s + 4k_s)]} \tag{42}$$

In high magnetic fields the expression for $\tilde{\rho}_{ST}(\sigma,r,s)$ is the same as 41, but with $3k_s$ replaced by k_s, and in the auxiliary function $\tilde{J}_c(r,s)$ the quantity $4k_s$ is replaced by $2k_s$.

Expressions 33−43 represent the closed set of equations allowing us to calculate the quantum yield of exciplex fluorescence $\overline{\eta}_e = (1 - \eta_f)\overline{\varphi}_e$, as well as the magnetic field effect χ_e within the Scheme II. In the present study these

dx.doi.org/10.1021/jp5070648 | J. Phys. Chem. C 2014, 118, 21365−21376

equations were solved numerically using the QM2L software package.[62]

These numerical results allow estimating an accuracy of the model used in Section IV. For example, the calculated $\overline{\varphi}_e(L)$ dependencies in weak and strong fields shown in Figure 2 (Panel B) give the values of the exciplex quantum yield both in close-to-contact charge separation processes (at $L \to 0$) and in distant reactions (at $L \geq 1$ Å). One can see that the ratio

$$\rho = \frac{\overline{\varphi}_e(1\text{Å}) - \overline{\varphi}_e(0.1\text{Å})}{\overline{\varphi}_e(1\text{Å})} \tag{43}$$

does not exceed a few percents both in low-field and high-field limits. Although the spatial distribution of RIPs formed in charge separation processes considerably changes with variation of L (see Figure 6A), its impact on the exciplex quantum yield

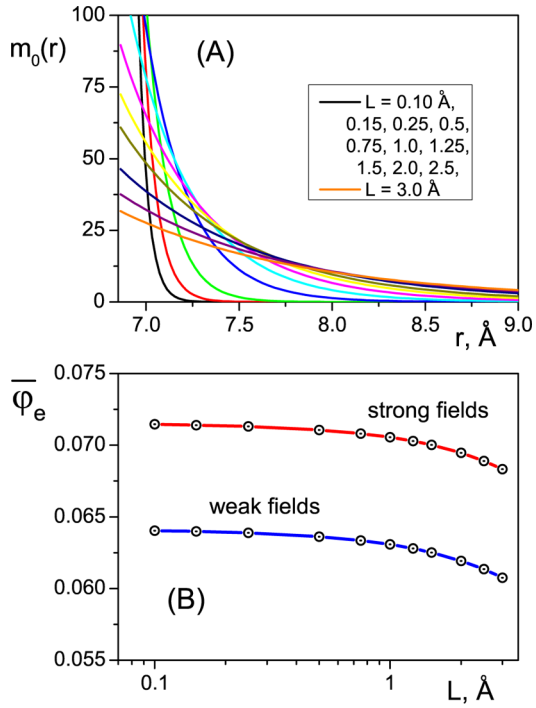

Figure 6. (A) Initial distributions of RIPs over the D^+–A^- distances in the Weller Scheme II (eq 34). Different colors correspond to different values of the electronic tunnelling length L (indicated on the graph). (B) The quantum yield of exciplex fluorescence, $\overline{\varphi}_e$, as a function of L in weak (blue) and strong (red) magnetic fields. The parameters are $k_b = 0$, $k_f = k_I(0) = 50\,000$ Å^3/ns, $\tau_A = 5$ ns, $\tau_e = 50$ ns, $k_s = 0.03$ ns^{-1}, $k_a = 15\,000$ Å^3/ns, $D = 250$ Å^2/ns, $\varepsilon = 37$, $\Delta G_{exc} = -0.2$ eV, and $\Delta G_I = -0.1$ eV.

is rather small. It should be pointed out that applicability of the contact approximation depends on model parameters rather strongly. For example, here the value of $K = 620$ Å^3/ns adopted for the chemical systems studied in ref 28 is exploited. An increase of association rate k_a results in a rise of the parameter ρ up to 100% at $K = 10^5$ Å^3/ns.

In most molecular systems the values of the electron tunnelling length L are known to lie in the range from 1 to 1.5 Å. However, the effective donor-to-acceptor distance in ET may depend not only on L but also on other factors like solvent polarity ε and the free energy of charge separation ΔG_I.[43,49] As for distribution of the ion pairs in highly polar solvents like acetonitrile ($\varepsilon \simeq 37$) it can be shifted out of the contact by several angstroms when $-\Delta G_I$ varies from 0 (resonant transfer, normal Marcus region) to $2E_{rm}$ (deep in the inverted Marcus region). That is why the accuracy of the contact approximation can depend critically on the ET regime (normal or inverted region).

We inspected this conclusion numerically within the present model and calculated the dependence of the exciplex magnetic field effect χ_e on the L parameter using different values of the ET free energy gap. The results are shown in Figure 7 where

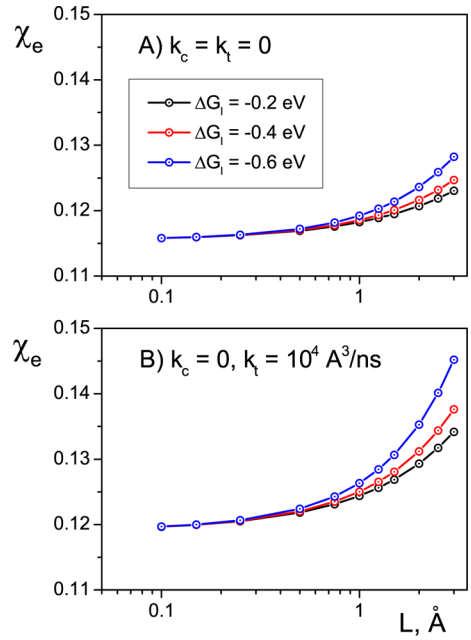

Figure 7. Magnetic-field effect on the exciplex, χ_e, as a function of the electronic tunnelling length L within the noncontact theory. The results in the upper and lower panels differ by the recombination rates k_t (indicated therein). Black, red, and blue curves correspond to $\Delta G_I = -0.2$, -0.4, and -0.6 eV, respectively. $\Delta G_I - \Delta G_{exc} = 0.1$ eV; other parameters are the same as in the Figure 6 caption.

the upper and the lower panels correspond to different values of the triplet RIP recombination rate, k_t, (indicated on the graph). The contact value of the solvent reorganization energy is taken to be the same for all the curves ($E_{rm}(\sigma) = 0.5$ eV), while the ΔG_I parameter is varied (-0.2, -0.4, and -0.6 eV) covering both the normal and the inverted Marcus regions. In all simulations the rate k_f was kept constant by adjusting the value of electronic coupling, V_0.

The results in Figure 7 clearly verify our previous assumption that contact approximation becomes more accurate for the low-exergonic charge separation reactions proceeding in the normal region (compare black and blue curves in the figure). Particularly, for nonrecombining RIPs ($k_t = k_c = 0$, the upper panel in Figure 7) the ratio ρ amounts to 0.021 for $\Delta G_I = -0.2$ eV and 0.029 for $\Delta G_I = -0.6$ eV. On the other hand, for the singlet-born RIPs subjected to recombination from the triplet state ($k_c = 0$, $k_t \neq 0$, the lower panel in Figure 7) the $\chi_e(L)$ dependence is more prominent, and the above ratio is 0.038 for $\Delta G_I = -0.2$ eV and 0.052 for $\Delta G_I = -0.6$ eV.

We should mention that results of the contact theory (eq 31) and of the remote-ET model (eqs 32–42) coincide only at large ε. Calculations show that inequality $\varepsilon > 80$ can be roughly used as a condition of close correspondence between the two models. Under this condition the results of the contact and

dx.doi.org/10.1021/jp5070648 | J. Phys. Chem. C 2014, 118, 21365–21376

noncontact theories (namely, the calculated χ_e values) do not differ more than 1%, but this coincidence quickly deteriorates for less polar solvents. Particularly, numerical simulations give the difference about 2.5% at $\varepsilon = 60$, 9.6% at $\varepsilon = 30$, and even 38% at $\varepsilon = 15$. Such strong deviations were caused by the restricted applicability of eq 40 which is accurate only for large ε.

VII. CONCLUDING REMARKS

In this paper a simple kinetic model of fluorescence quenching by electron transfer is developed. It incorporates the reactants, products, and intermediates: the fluorophore in its ground state, singlet and triplet excited states, as well as the exciplex and the RIP in its singlet and triplet spin states. The reversible transitions between these species are described in terms of monomolecular and bimolecular rate constants. The spatial motion of the particles in solution is modeled by continuous diffusion influenced by the Coulomb interaction of the charged particles. The rate of the spin transitions between the singlet and triplet states of geminate RIPs is magnetic-sensitive that leads to the MFE on both the fluorophore and the exciplex. The close analytic expressions for the MFEs are obtained.

A close similarity of the MFE behaviors for the Schemes I and II is the main output of this study. The magnitudes of χ_f and χ_e as well as their dependencies on many model parameters are found to be qualitatively the same in both the reaction schemes. There is however a single parameter that violates this regularity. This is the rate constant of the RIP-to-exciplex association k_a. The $\chi_f(k_a)$ and $\chi_e(k_a)$ dependencies are found to be opposite for the Schemes I and II that give some opportunities for differentiation between the RIP and exciplex formation processes in photochemical systems.

AUTHOR INFORMATION

Corresponding Author

*E-mail: anatoly.ivanov@volsu.ru.

Notes

The authors declare no competing financial interest.

ACKNOWLEDGMENTS

This work was supported by the Russian Foundation for Basic Research (grants 14-03-00261 and 14-07-97028).

REFERENCES

(1) Marcus, R. A. On the Theory of Oxidation-Reduction Reactions Involving Electron Transfer. I. *J. Chem. Phys.* **1956**, *24*, 966−978.
(2) Zusman, L. D. Outer-Sphere Electron Transfer in Polar Solvents. *Chem. Phys.* **1980**, *49*, 295−304.
(3) Marcus, R. A.; Sutin, N. Electron Transfers in Chemistry and Biology. *Biochim. Biophys. Acta, Rev. Bioenerg.* **1985**, *811*, 265−322.
(4) Kuznetsov, A. M. *Charge Transfer in Physics, Chemistry and Biology*; Gordon & Breach: Amsterdam, 1995.
(5) Electron Transfer: From Isolated Molecules to Biomolecules, In *Adv. Chem. Phys.*; Jortner, J., Bixon, M., Ed.; Wiley: New York, 1999; Vol. *106*, *107*.
(6) Bullock, J. E.; Carmieli, R.; Mickley, S. M.; Vura-Weis, J.; Wasielewski, M. R. Photoinitiated Charge Transport through p-Stacked Electron Conduits in Supramolecular Ordered Assemblies of Donor-Acceptor Triads. *J. Am. Chem. Soc.* **2009**, *131*, 11919−11929.
(7) Wasielewski, M. R. Self-Assembly Strategies for Integrating Light Harvesting and Charge Separation in Artificial Photosynthetic Systems. *Acc. Chem. Res.* **2009**, *42*, 1910−1921.
(8) Heeger, A. J. Semiconducting Polymers: the Third Generation. *Chem. Soc. Rev.* **2010**, *39*, 2354−2371.
(9) Bhosale, R.; Misek, J.; Sakai, N.; Matile, S. Supramolecular n/p-heterojunction Photosystems with Oriented Multicolored Antiparallel Redox Gradients (OMARG-SHJs). *Chem. Soc. Rev.* **2010**, *39*, 138−149.
(10) Dimitrov, S. D.; Bakulin, A. A.; Nielsen, C. B.; Schroeder, B. C.; Du, J.; Bronstein, H.; McCulloch, I.; Friend, R. H.; Durrant, J. R. On the Energetic Dependence of Charge Separation in Low-Band-Gap Polymer/Fullerene Blends. *J. Am. Chem. Soc.* **2012**, *134*, 18189−18192.
(11) Weller, A. Exciplex and Radical Pairs in Photochemical Electron Transfer. *Pure Appl. Chem.* **1982**, *54*, 1885−1888.
(12) Masuhara, H.; Mataga, N. Ionic Photodissociation of Electron Donor-Acceptor Systems in Solution. *Acc. Chem. Res.* **1981**, *14*, 312−318.
(13) Kikuchi, K.; Niwa, T.; Takahashi, Y.; Ikeda, H.; Miyashi, T.; Hoshi, M. Evidence of Exciplex Formation in Acetonitrile. *Chem. Phys. Lett.* **1990**, *173*, 421−424.
(14) Kikuchi, K. A New Aspect of Photoinduced Electron Transfer in Acetonitrile. *J. Photochem. Photobiol., A* **1992**, *65*, 149−156.
(15) Inada, T.; Kikuchi, K.; Takahashi, Y.; Ikeda, H.; Miyashi, T. Electron-Transfer (ET) Fluorescence Quenching in Benzonitrile. Evidence of an Intermolecular ET with $\Delta G < -0.5$ eV being a Diffusion-Controlled Process. *J. Phys. Chem. A* **2002**, *106*, 4345−4349.
(16) Mohammed, O. F.; Adamczyk, K.; Banerji, N.; Dreyer, J.; Lang, B.; Nibbering, E. T. J.; Vauthey, E. Direct Femtosecond Observation of Tight and Loose Ion Pairs upon Photoinduced Bimolecular Electron Transfer. *Angew. Chem., Int. Ed.* **2008**, *47*, 9044−9048.
(17) Frankevich, E. L.; Petrov, N. Kh. Magnetic Modulation of Fluorescence Intensity as a Method of Exploration of Reactions with Participation of Paramagnetic Particles. *Izv. Akad. Nauk SSSR, Ser. Fiz.* **1980**, *44*, 754−758.
(18) Kattnig, D. R.; Rosspeintner, A.; Grampp, G. Fully Reversible Interconversion between Locally Excited Fluorophore, Exciplex, and Radfical Ion Pair Demonstrated by a New Magnetic Field Effect. *Angew. Chem., Int. Ed.* **2008**, *47*, 960−962.
(19) Salikhov, K. M.; Molin, Y. N.; Sagdeev, R. Z.; Buchachenko, A. L. *Spin Polarization and Magnetic Effects in Radical Reactions*; Elsiever: Amsterdam, 1984.
(20) Steiner, U. E.; Ulrich, Th. Magnetic Field Effect in Chemical Kinetics and Related Phenomena. *Chem. Rev.* **1989**, *89*, 51−147.
(21) McLauchlan, K. A.; Steiner, U. E. The Spin-Correlated Radical Pair as a Reaction Intermediate. *Mol. Phys.* **1991**, *73*, 241−263.
(22) Brocklehurst, B. Magnetic Fields and Radical Reactions: Recent Developments and Their Role in Nature. *Chem. Soc. Rev.* **2002**, *31*, 301−311.
(23) Lukzen, N. N.; Kattnig, D. R.; Grampp, G. The Effect of Signs of Hyperfine Coupling Constant on MARY Spectra Affected by Degenerate Electron Exchange. *Chem. Phys. Lett.* **2005**, *413*, 118−122.
(24) Justinek, V.; Grampp, G.; Landgraf, S.; Hore, P. J.; Lukzen, N. N. Electron Self-Exchange Kinetics Determined by MARY Spectroscopy: Theory and Experiment. *J. Am. Chem. Soc.* **2004**, *126*, 5635−5646.
(25) Nath, D. N.; Chowdhury, M. Effect of Variation of Dielectric Constant on the Magnetic Field Modulation of Exciplex Luminescence. *Pramana J. Phys.* **1990**, *34*, 51−66.
(26) Ivanov, A. I.; Burshtein, A. I. The Double-Channel Contact Recombination and Separation of Geminate Radical Ion Pairs in a Coulomb Well. *J. Phys. Chem. A* **2008**, *112*, 6392−6397.
(27) Dodin, D. V.; Ivanov, A. I.; Burshtein, A. I. Noncontact Bimolecular Photoionization Followed by Radical-Ions Separation and Their Geminate Recombination Assisted by Coherent HFI Induced Spin-Conversion. *J. Phys. Chem. A* **2008**, *112*, 889−897.
(28) Kattnig, D. R.; Rosspeintner, A.; Grampp, G. Magnetic Field Effects on Exciplex-Forming Systems: the Effect on the Locally Excited Fluorophore and its Dependence on Free Energy. *Phys. Chem. Chem. Phys.* **2011**, *13*, 3446−3460.
(29) Werner, H.-J.; Schulten, Z.; Schulten, K. Theory of the Magnetic Field Modulated Geminate Recombination of Radical Ion Pairs in

Polar Solvents: Application to the Pyreneï-N,N-dimethylaniline System. *J. Chem. Phys.* **1977**, *67*, 646−663.
(30) Tanimoto, Y.; Hasegawa, K.; Okada, N.; Itoh, M.; Iwai, K.; Sugioka, K.; Takemura, F.; Nakagaki, R.; Nagakura, S. Magnetic Field Effects on the Intra- and Intermolecular Exciplex Fluorescence of Phenanthrene and Dimethylaniline. *J. Phys. Chem.* **1989**, *93*, 3586−3594.
(31) Petrov, N. Kh.; Borisenko, V. N.; Alfimov, M. V.; Fiebig, T.; Staerk, H. Fluorescence-Detected Magnetic Field Effects in Exciplex Systems Containing Azacrown Ethers as Electron Donor. *J. Phys. Chem.* **1996**, *100*, 6368−6370.
(32) Weller, A. Mechanism and Spindynamics of Photoinduced Electron Transfer Reactions. *Z. Phys. Chem., Neue Folge* **1982**, *130*, 129−138.
(33) Weller, A.; Staerk, H.; Treichel, R. Magnetic-Field Effects on Geminate Radical-Pair Recombination. *Faraday Discuss. Chem. Soc.* **1984**, *78*, 271−278.
(34) Arnold, B. R.; Noukakis, D.; Farid, S.; Goodman, J. L.; Gould, I. R. Dynamics of Interconversion of Contact and Solvent-Separated Radical-Ion Pairs. *J. Am. Chem. Soc.* **1995**, *117*, 4399−4400.
(35) Kikuchi, K.; Takahashi, Y.; Katagiri, T.; Niwa, T.; Hoshi, M.; Miyashi, T. A Critical Consideration on the Lack of Inverted Region in the Rehmï-Weller Plot for Electron-Transfer Fluorescence Quenching. *Chem. Phys. Lett.* **1991**, *180*, 403−408.
(36) Gould, I. R.; Young, R. H.; Mueller, L. J.; Farid, S. Mechanisms of Exciplex Formation. Roles of Superexchange, Solvent Polarity, and Driving Force for Electron Transfer. *J. Am. Chem. Soc.* **1994**, *116*, 8176−8187.
(37) Nath, D. N.; Chowdhury, M. Effect of Environment on the Magnetic Field Modulation of Exciplex Luminescence. *Chem. Phys. Lett.* **1984**, *109*, 13−17.
(38) Richert, S.; Rosspeintner, A.; Landgraf, S.; Grampp, G.; Vauthey, E.; Kattnig, D. R. Time-Resolved Magnetic Field Effects Distinguish Loose Ion Pairs from Exciplexes. *J. Am. Chem. Soc.* **2013**, *135*, 15144−15152.
(39) Koch, M.; Letrun, R.; Vauthey, E. Exciplex Formation in Bimolecular Photoinduced Electron-Transfer Investigated by Ultrafast Time-Resolved Infrared Spectroscopy. *J. Am. Chem. Soc.* **2014**, *136*, 4066−4074.
(40) Dodin, D. V.; Ivanov, A. I.; Burshtein, A. I. Magnetic Field Effect in Fluorescence of Excited Fluorophore Equilibrated with Exciplex that Reversibly Dissociates into Radical-Ion Pair Undergoing the Spin Conversion. *J. Chem. Phys.* **2012**, *137*, 024511−1−6.
(41) Dodin, D. V.; Ivanov, A. I.; Burshtein, A. I. Hyperfine Interaction Mechanism of Magnetic Field Effects in Sequential Fluorophore and Exciplex Fluorescence. *J. Chem. Phys.* **2013**, *138*, 124102−1−11.
(42) Burshtein, A. I.; Ivanov, A. I. Diffusion Affected Magnetic Field Effect in Exciplex Fluorescence. *J. Chem. Phys.* **2014**, *141*, 024508−1−5.
(43) Burshtein, A. I. Non-Markovian Theories of Transfer Reactions in Luminescence and Chemiluminescence and Photo- and Electrochemistry. *Adv. Chem. Phys.* **2004**, *129*, 105−418.
(44) Gorelik, E. V.; Lukzen, N. N.; Sagdeev, R. Z.; Steiner, U. E. Application of Integral Encounter Theory to Account for the Spin Effects in Radical Reactions I. Δg and Spin Relaxation Effects on Recombination Kinetics of Free Radicals. *Chem. Phys.* **2000**, *262*, 303−323.
(45) Burshtein, A. I.; Ivanov, K. L. The Crucial Role of Triplets in Photoinduced Charge Transfer and Separation. *Phys. Chem. Chem. Phys.* **2002**, *4*, 4115−4125.
(46) Ivanov, A. I.; Burshtein, A. I. Luminescence Quenching by Reversible Ionization or Exciplex Formation/Dissociation. *J. Phys. Chem. A* **2008**, *112*, 11547−11558.
(47) Petrova, M. V.; Burshtein, A. I. Reversible Exciplex Formation Followed Charge Separation. *J. Phys. Chem. A* **2008**, *112*, 13343−13351.
(48) Jana, A. K.; Roy, P.; Nath, D. N. Role of Viscosity in the Magnetic Field Effect on Pyrene−DMA Exciplex Emission at Different Permittivities. *Chem. Phys. Lett.* **2014**, *593*, 145−149.
(49) Burshtein, A. I. Unified Theory of Photochemical Charge Separation. *Adv. Chem. Phys.* **2000**, *114*, 419−587.
(50) Burshtein, A. I.; Lukzen, N. N. Reversible Reactions of Metastable Reactants. *J. Chem. Phys.* **1995**, *103*, 9631−9641.
(51) Burshtein, A. I.; Yakobson, B. I. A Modified Model of Diffusion-Controlled Reactions. *Int. J. Chem. Kinet.* **1980**, *12*, 261−270.
(52) Burshtein, A. I.; Doktorov, A. B.; Morozov, V. A. Contact Reactions of Randomly Walking Particles. Rotational Averaging of Chemical Anisotropy. *Chem. Phys.* **1986**, *104*, 1−18.
(53) Kuzmin, M. G. Exciplex Mechanism of Excited State Electron Transfer Reactions in Polar Media. *J. Photochem. Photobiol. A: Chem.* **1996**, *102*, 51−57.
(54) Dogadkin, D. N.; Soboleva, I. V.; Kuzmin, M. G. Formation Enthalpy and Entropy of Exciplexes with Variable Extent of Charge Transfer in Solvents of Different Polarity. *High Energy Chem.* **2001**, *35*, 251−257.
(55) Arnold, B. R.; Farid, S.; Goodman, J. L.; Gould, I. R. Absolute Energies of Interconverting Contact and Solvent-Separated Radical-Ion Pairs. *J. Am. Chem. Soc.* **1996**, *118*, 5482−5483.
(56) Zharikov, A. A.; Shokhirev, N. V. The Influence of Solvent Polarity and Viscosity on Magnetic Effects in Geminate Recombination. Balance Approximation. *Z. Phys. Chem.* **1992**, *177*, 37−61.
(57) Knibbe, H.; Rehm, D.; Weller, A. Intermediants and Kinetics of Fluorescence Quenching by Electron Transfer. *Ber. Bunsen-Ges. Phys. Chem.* **1968**, *72*, 257−262.
(58) Werner, H.-J.; Staerk, H.; Weller, A. Solvent, Isotope, and Magnetic Field Effects in the Geminate Recombination of Radical Ion Pairs. *J. Chem. Phys.* **1978**, *68*, 2419−2426.
(59) Shushin, A. I. Magnetic Field Effects in Radical Pair Recombination. I. CIDNP and CIDEP in Geminate Recombination. *Chem. Phys.* **1990**, *144*, 201−222.
(60) Shushin, A. I. The Time Dependent Solution of the Smoluchowski Equation: Kinetics of Escaping from the Well for Different Dimensionalities. *J. Chem. Phys.* **1991**, *95*, 3657−3665.
(61) Fedorenko, S. G. Two-State Model of Excess Electron Relaxation and Geminate Recombination in Water and Aqueous Solutions. *Chem. Phys.* **2010**, *371*, 43−54.
(62) Gladkikh, V.; Burshtein, A. I.; Feskov, S. V.; Ivanov, A. I.; Vauthey, E. Hot Recombination of Photogenerated Ion Pairs. *J. Chem. Phys.* **2005**, *123*, 244510−1−11.